ISE

Industrial and
Systems Engineering

Conformal Symplectic and Relativistic Optimization

GUILHERME FRANÇA[1,2], JEREMIAS SULAM[2], DANIEL P. ROBINSON[3], AND RENÉ VIDAL[2]

[1]Computer Science Division, University of California, Berkeley

[2]Mathematical Institute for Data Science, Johns Hopkins University

[3]Department of Industrial and Systems Engineering, Lehigh University

ISE Technical Report 19T-022

LEHIGH
UNIVERSITY

Conformal Symplectic and Relativistic Optimization

Guilherme França,[a,b,*] Jeremias Sulam,[b] Daniel P. Robinson,[c] and René Vidal[b]

[a] *Computer Science Division, University of California, Berkeley*
[b] *Mathematical Institute for Data Science, Johns Hopkins University*
[c] *Industrial and Systems Engineering, Lehigh University*

Abstract

Arguably the most popular accelerated or momentum-based optimization methods are Nesterov's accelerated gradient and Polyaks's heavy ball, both corresponding to different discretizations of a particular second order differential equation. Such connections with continuous-time dynamical systems have been instrumental in demystifying acceleration phenomena in optimization. Recently, symplectic techniques started to attract interest in this context since they are known to preserve important structural properties of the continuous system, such as critical points, stability, and even convergence rates. Here we study structure-preserving discretizations for a certain class of dissipative (conformal) Hamiltonian systems, allowing us to analyze the symplectic structure of both Nesterov and heavy ball besides providing several new insights into these methods. Moreover, we propose a new algorithm based on a dissipative relativistic system that normalizes the momentum and may result in more stable/faster optimization. Importantly, such a method generalizes both Nesterov's and heavy ball, each being recovered as distinct limiting cases, and has potential advantages at no additional cost.

Contents

[*] guifranca@gmail.com

1 Introduction

Gradient based optimization methods are ubiquitous in machine learning since they only require first order information on the objective function. This makes them computationally efficient. However, vanilla gradient descent can be slow. Alternatively, *accelerated gradient methods*, whose construction can be traced back to Polyak [1] and Nesterov [2], became popular due to their ability to achieve best worst-case complexity bounds. The heavy ball method, also known as *classical momentum* (CM) method, is given by

$$v_{k+1} = \mu v_k - \epsilon \nabla f(x_k), \qquad x_{k+1} = x_k + v_{k+1}, \tag{1.1}$$

where $\mu \in (0,1)$ is the momentum factor, $\epsilon > 0$ the learning rate, and $f : \mathbb{R}^n \to \mathbb{R}$ the function being minimized. Similarly, *Nesterov's accelerated gradient* (NAG) can be found in the form

$$v_{k+1} = \mu v_k - \epsilon \nabla f(x_k + \mu v_k), \qquad x_{k+1} = x_k + v_{k+1}. \tag{1.2}$$

Both methods have a long history in optimization and machine learning [3]. They are also the basis of other methods such as adaptive ones that additionally include some gradient normalization [4–7].

In discrete-time optimization the "acceleration phenomena" are considered counterintuitive. However, a promising direction has been emerging in connection with continuous-time dynamical systems—see e.g. [8–18]—where many of these difficulties disappear or have an intuitive explanation. Since one is free to discretize a continuous system in many different ways, it is only natural to ask which discretization strategies would be most suitable for optimization? Such a question is unlikely to have a simple answer, and may be problem dependent. Unfortunately, typical discretizations are also known to introduce spurious artifacts and do not reproduce the most important properties of the system [19]. Nevertheless, a special class of discretizations in the physics literature known as *symplectic integrators* [19–22] are known to be preferable whenever considering a *conservative* Hamiltonian system.

More relevant to optimization is a class of *dissipative systems* known as *conformal Hamiltonian systems* [23]. Recently, results from symplectic integrators were extended to this class and such methods are called *conformal symplectic integrators* [24]. Conformal symplectic methods tend to have long time stability because the numerical trajectories remain in the same conformal symplectic manifold as the original continuous system [18]. Importantly, these methods do not change the phase portrait of the system, i.e., the stability of critical points is preserved. Although symplectic techniques have had great success in several areas of physics and Monte Carlo methods, only very recently they started to be considered in optimization [14, 18] and are still mostly unexplored in this context.

In this paper, we *relate conformal symplectic integrators to optimization* and provide important insights into CM (1.1) and NAG (1.2). We prove that CM is a first order accurate conformal symplectic integrator. On the other hand, NAG is also first order accurate but not conformal symplectic since it introduces some spurious dissipation, or excitation. However,

Algorithm 1 *Relativistic gradient descent* (RGD) for minimizing $f(x)$. (In practice, we recommend setting $\alpha = 1$ which results in a conformal symplectic method.)

```
Require: Initial state $(x_0, v_0)$ and parameters $\epsilon > 0$ (step size), $\delta > 0$, $\mu \in (0,1)$, $\alpha \in [0,1]$
  for $k = 0, 1, \dots$ do
    $x_{k+1/2} \leftarrow x_k + \sqrt{\mu}\, v_k \big/ \sqrt{\mu\delta\|v_k\|^2 + 1}$
    $v_{k+1/2} \leftarrow \sqrt{\mu} v_k - \epsilon \nabla f(x_{k+1/2})$
    $x_{k+1} \leftarrow \alpha x_{k+1/2} + (1-\alpha) x_k + v_{k+1/2} \big/ \sqrt{\delta\|v_{k+1}\|^2 + 1}$
    $v_{k+1} \leftarrow \sqrt{\mu}\, v_{k+1/2}$
  end for
```

it does so in an interesting way that depends on the Hessian $\nabla^2 f$; the symplectic form contracts in a Hessian dependent manner and so do phase space volumes. This is an effect of higher order but can influence the behaviour of the algorithm. We also derive modified equations and shadow Hamiltonians for both CM and NAG. Moreover, we indicate a tradeoff between stability, symplecticness, and such an spurious contraction, suggesting advantages in structure-preserving discretizations for optimization.

Optimization can be challenging in a landscape with large gradients, e.g., for a function with fast growing tails. The only way to control divergences in methods such as (1.1) and (1.2) is to make the step size ϵ very small, but then the algorithm becomes slow. One approach to this issue is to introduce a suitable normalization of the gradient. Here we propose an alternative approach motivated by special relativity in physics. The reason is that in special relativity there is a limiting speed—the speed of light. Thus, by discretizing a dissipative relativistic system we obtain an algorithm that incorporates this effect and may result in more stable optimization in settings with large gradients. Specifically, we introduce Algorithm 1. Besides the momentum factor μ and the learning rate ϵ, already present in (1.1) and (1.2), the RGD method have two additional parameters, $\delta \ge 0$ and $0 \le \alpha \le 1$, which brings some interesting properties:

- When $\delta = 0$ and $\alpha = 0$, RGD recovers NAG (1.2). When $\delta = 0$ and $\alpha = 1$, RGD becomes a second order accurate version of CM (1.1), which has similar behavior but is more stable. Thus, RGD can interpolate between these two methods. Moreover, RGD has the same computational cost as CM and NAG, thus being at least as efficient as these methods—if appropriately tuned.

- Let $y_k \equiv \alpha x_{k+1/2} + (1-\alpha)x_k$. The last update in Algorithm 1 implies $\|x_{k+1} - y_k\| \le 1/\delta$. Thus with $\delta > 0$ RGD is globaly bounded regardless how large $\|\nabla f\|$ might be; this is in contrast with CM and NAG where $\delta = 0$. The square root factor in Algorithm 1 has a "relativistic origin" and its strength is controlled by δ. For this reason, RGD may be more stable compared to CM or NAG—see Fig. 3 in Appendix C—and potentially preventing divergences in settings of large gradients.

- As we will show, $\alpha = 1$ implies that RGD is *conformal symplectic*, whereas $\alpha = 0$

implies a spurious Hessian driven damping similarly found in NAG. Thus, RGD has the flexibility of being "dissipative-preserving" or introducing some extra "spurious contraction." However, based on theoretical arguments and empirical evidence, we advocate for the choice $\alpha = 1$.[1]

We mention few related works. Applications of symplectic integrators in optimization was first considered in [14]—although this is different than the conformal symplectic case explored here. Recently, the benefits of symplectic methods in optimization started to be indicated [25]. Actually, even more recently a generalization of symplectic methods to dissipative cases was proposed [18], showing that such methods may be "rate-preserving" up to a negligible error—this construction is more general and contains the conformal symplectic case as a particular case. Relativistic systems are obviously an elementary topic in physics, but—with some modifications—the relativistic kinetic energy was considered in Monte Carlo methods [26, 27] and also briefly in [28]. Finally, let us stress that Algorithm 1 is a completely new method in the literature, generalizing perhaps the two most popular existing accelerated methods, namely CM and NAG, and also having the ability to be conformal symplectic besides being adaptive in the momentum which may help controlling divergences.

2 Conformal Hamiltonian Systems

We start with the basics of conformal Hamiltonian systems and focus on their intrinsic symplectic geometry; we refer to [23] for details. The state of the system is described by a point on phase space, $(x, p) \in \mathbb{R}^{2n}$, where $x = x(t)$ is the generalized coordinates and $p = p(t)$ its conjugate momentum, with $t \in \mathbb{R}$ being the time. The system is completely specified by a Hamiltonian $H : \mathbb{R}^{2n} \to \mathbb{R}$ and required to obey a modified form of Hamilton's equations:

$$\dot{x} = \nabla_p H(x, p), \qquad \dot{p} = -\nabla_x H(x, p) - \gamma p. \tag{2.1}$$

Here $\dot{x} \equiv \frac{dx}{dt}$, $\dot{p} \equiv \frac{dp}{dt}$, and $\gamma > 0$ is a constant. A classical example is

$$H(x, p) = \frac{\|p\|^2}{2m} + f(x) \tag{2.2}$$

where $m > 0$ is the mass of a particle subject to a potential f. The Hamiltonian is the energy of the system and upon taking its time derivative one finds $\dot{H} = -\gamma \|p\|^2 \le 0$. Thus, H is a Lyapunov function and all orbits tend to fixed points, which in this case must satisfy $\nabla f(x) = 0$ and $p = 0$. This implies that the system is stable on isolated minimizers of f. (This can actually be generalized under the assumption that H is any strongly convex function of p with minimum at $p = 0$.)

[1] The only reason for introducing this extra parameter $0 \le \alpha \le 1$ into Algorithm 1 is to actually let the experiments decide whether $\alpha = 1$ (symplectic) or $\alpha < 1$ (non symplectic) is desirable or not.

Define

$$z \equiv \begin{bmatrix} x \\ p \end{bmatrix}, \qquad \Omega \equiv \begin{bmatrix} 0 & I \\ -I & 0 \end{bmatrix}, \qquad D \equiv \begin{bmatrix} 0 & 0 \\ 0 & I \end{bmatrix}, \tag{2.3}$$

where I is the $n \times n$ identity matrix, to write the equations of motion (2.1) concisely as[2]

$$\dot{z} = \underbrace{\Omega \nabla H(z)}_{C(z)} - \underbrace{\gamma D z}_{D(z)}. \tag{2.4}$$

Note that $\Omega\Omega^T = \Omega^T\Omega = I$ and $\Omega^2 = -I$, so that Ω is real, orthogonal and antisymmetric. Let $\xi, \eta \in \mathbb{R}^{2n}$ and define the *symplectic 2-form* $\omega(\xi, \eta) \equiv \xi^T \Omega\, \eta$. It is convenient to use the wedge product representation of this 2-form, namely[3]

$$\omega(\xi, \eta) = (dx \wedge dp)(\xi, \eta). \tag{2.5}$$

We denote $\omega_t \equiv dx(t) \wedge dp(t)$. The equations of motion define a flow $\Phi_t : \mathbb{R}^{2n} \to \mathbb{R}^{2n}$, i.e. $\Phi_t\big(z_0\big) \equiv z(t)$ where $z(0) \equiv z_0$. Let $J_t(z)$ denote the Jacobian of $\Phi_t(z)$. From (2.4) it is not hard to show that (see e.g. [23])

$$J_t^T \Omega J_t = e^{-\gamma t}\Omega \qquad \Longrightarrow \qquad \omega_t = e^{-\gamma t}\omega_0. \tag{2.6}$$

Therefore, a conformal Hamiltonian flow Φ_t *contracts the symplectic form exponentially* with respect to the damping coefficient γ. It follows from (2.6) that volumes on phase space shrink as $\operatorname{vol}(\Phi_t(\mathcal{R})) = \int_{\mathcal{R}} |\det J_t(z)| dz = e^{-n\gamma t} \operatorname{vol}(\mathcal{R})$ where $\mathcal{R} \subset \mathbb{R}^{2n}$. This contraction is stronger as dimension increases. The conservative case is recovered with $\gamma = 0$ above; in this case, the symplectic structure is preserved and volumes remain invariant (Liouville's theorem). A known and interesting property of conformal Hamiltonian systems is that their Lyapunov exponents sum up in pairs to γ [31]. This imposes constraints on the admissible dynamics and controls the phase portrait near fixed points. For other properties of attractor sets we refer to [32]. Finally, conformal symplectic transformations can be composed and form the so-called conformal group.

3 Conformal Symplectic Optimization

Consider (2.4) where we associate flows Φ_t^C and Φ_t^D to the respective vector fields $C(z)$ and $D(z)$. Conformal symplectic integrators can be constructed as *splitting methods* that approximate the true flow Φ_t by composing the individual flows Φ_t^C and Φ_t^D. Our procedure to obtain a numerical map Ψ_h, with step size $h > 0$, is to first obtain a numerical approximation

[2] $C(z)$ and $D(z)$ will be used later on and stand for "conservative" and "dissipative" parts, respectively.

[3] It is not strictly necessary to be familiar with differential forms and exterior calculus to understand this paper. For the current purposes, it is enough to recall that the wedge product is a bilinear and antisymmetric operation, i.e. $dx \wedge (a dy + b dz) = a dx \wedge dy + b dx \wedge dz$ and $dx \wedge dy = -dy \wedge dx$ for scalars a and b and 1-forms dx, dy, dz (think about this as vector differentials); we refer to [29] and [30] for more details if necessary.

to the conservative part of the system, $\dot{z} = \Omega \nabla H(z)$. This yields a numerical map Ψ_h^C that approximates Φ_h^C for small intervals of time $[t, t+h]$. One can choose any standard *symplectic integrator* for this task. Let us pick the simplest, i.e. the symplectic Euler method [30, pp. 189]. We thus have $\Psi_h^C : (x, p) \mapsto (X, P)$ where

$$X = x + h\nabla_p H(x, P), \qquad P = p - h\nabla_x H(x, P). \tag{3.1}$$

Now the dissipative part of the system, $\dot{z} = -\gamma D z$, can be integrated exactly. Indeed, $\dot{q} = 0$ and $\dot{p} = -\gamma p$, thus $\Psi_h^D : (x, p) = (x, e^{-\gamma h} p)$. With the composition $\Psi_h \equiv \Psi_h^C \circ \Psi_h^D$ we obtain $\Psi_h : (x, p) \mapsto (X, P)$ as

$$P = e^{-\gamma h} p - h\nabla_x H(x, P), \qquad X = x + h\nabla_p H(x, P). \tag{3.2}$$

This is nothing but a *dissipative version* of the symplectic Euler method. Similarly, if we choose the leapfrog method [30, pp. 190] for Ψ_h^C and consider $\Psi_h \equiv \Psi_{h/2}^D \circ \Psi_h^C \circ \Psi_{h/2}^D$ we obtain

$$\tilde{X} = x + (h/2)\nabla_p H\big(\tilde{X}, e^{-\gamma h/2} p\big), \tag{3.3a}$$

$$\tilde{P} = e^{-\gamma h/2} p - (h/2)\big(\nabla_x H\big(\tilde{X}, e^{-\gamma h/2} p\big) + \nabla_x H\big(\tilde{X}, \tilde{P}\big)\big), \tag{3.3b}$$

$$X = \tilde{X} + (h/2)\nabla_p H(\tilde{X}, \tilde{P}), \tag{3.3c}$$

$$P = e^{-\gamma h/2} \tilde{P}. \tag{3.3d}$$

This is a *dissipative* version of the leapfrog, which is recovered when $\gamma = 0$. Note that in general (3.2) is implicit in P, and (3.3) is implicit in $\tilde{X}$ and P. However, both will become explicit for separable Hamiltonians, $H = T(p) + f(x)$, and in this case they are extremely efficient. Note also that (3.2) and (3.3) are completely general, i.e. by choosing a suitable Hamiltonian H one can obtain several possible optimization algorithms from these integrators. Next, we show important properties of these integrators. (Below we denote $t_k = kh$ for $k = 0, 1, \ldots,$ $z_k \equiv z(t_k)$, etc.)

Definition 3.1. *A numerical map Ψ_h is said to be of order $r \geq 1$ if $\|\Psi_h(z) - \Phi_h(z)\| = O(h^{r+1})$ for any $z \in \mathbb{R}^{2n}$. (Recall that $h > 0$ is the step size and Φ_h the true flow.)*

Definition 3.2. *A numerical map Ψ_h is said to be conformal symplectic if $z_{k+1} = \Psi_h(z_k)$ is conformal symplectic, i.e. $\omega_{k+1} = e^{-\gamma h}\omega_k$, whenever $\hat{\Phi}_h$ is applied to a smooth Hamiltonian. Iterating such a map yields $\omega_k = e^{-\gamma t_k}\omega_0$ so that the contraction of the symplectic form (2.6) is preserved.*

Theorem 3.3. *Both methods (3.2) and (3.3) are conformal symplectic.*

Proof. Note that in both cases Ψ_h^C is a symplectic integrator, i.e. its Jacobian J_h^C obeys $(J_h^C)^T \Omega J_h^C = \Omega$ (see (2.6) with $\gamma = 0$). Now the map Ψ_h^D defined above is conformal symplectic, i.e. one can verify that its Jacobian J_h^D obeys $(J_h^D)^T \Omega J_h^D = e^{-\gamma h}\Omega$. Hence, any composition of these maps will be conformal symplectic. For instance:

$$(J_h^C J_h^D)^T \Omega (J_h^C J_h^D) = (J_h^D)^T (J_h^C)^T \Omega J_h^C J_h^D = (J_h^D)^T \Omega J_h^D = e^{-\gamma h}\Omega. \tag{3.4}$$

The same would be true for any type of composition whose overall timestep add up to h. □

Theorem 3.4. *The numerical scheme* (3.2) *is of order* $r = 1$*, while* (3.3) *is of order* $r = 2$*.*

Proof. The proof simply involves manipulating Taylor expansions for the numerical method and the continuous system over a time interval of h; this is presented in Appendix A. □

We mention that one can construct higher order integrators by following the above approach, however these would be more expensive, involving more gradient computations per iteration. In practice, methods of order $r = 2$ tend to have the best cost benefit.

4 Symplectic Structure of Heavy Ball and Nesterov

Consider the classical Hamiltonian (2.2) and replace into (3.2) to obtain:

$$p_{k+1} = e^{-\gamma h} p_k - h \nabla f(x_k), \qquad x_{k+1} = x_k + \tfrac{h}{m} p_{k+1}, \tag{4.1}$$

where we now make the iteration number $k = 0, 1, \dots$ explicit for convenience of the reader in relating to optimization methods. Introducing a change of variables:

$$v_k \equiv \tfrac{h}{m} p_k, \qquad \epsilon \equiv \tfrac{h^2}{m}, \qquad \mu \equiv e^{-\gamma h}, \tag{4.2}$$

we see that (4.1) is precisely the well-known CM method (1.1). Therefore, CM is nothing but a dissipative version of the symplectic Euler method. As a consequence of Theorems 3.3 and 3.4 we have:

Corollary 4.1. *The classical momentum method* (1.1) *is a conformal symplectic integrator for the Hamiltonian system* (2.2)*. Moreover, it is an integrator of order* $r = 1$*.*

Consider again the Hamiltonian (2.2) but replaced into (3.3). Let us also replace the last update (3.3d), i.e. from a previous iteration, into the first update (3.3a)—note that it is valid to replace successive updates without changing the algorithm. Thus, we obtain:

$$x_{k+1/2} = x_k + \tfrac{h}{2m} e^{-\gamma h} p_k, \quad p_{k+1} = e^{-\gamma h} p_k - h \nabla f(x_{k+1/2}), \quad x_{k+1} = x_{k+1/2} + \tfrac{h}{2m} p_{k+1}. \tag{4.3}$$

Define

$$v_k \equiv \tfrac{h}{2m} p_k, \qquad \epsilon \equiv \tfrac{h^2}{2m}, \qquad \mu \equiv e^{-\gamma h}, \tag{4.4}$$

to write (4.3) as

$$x_{k+1/2} = x_k + \mu v_k, \qquad v_{k+1} = \mu v_k - \epsilon \nabla f(x_{k+1/2}), \qquad x_{k+1} = x_{k+1/2} + v_{k+1}. \tag{4.5}$$

The reader can immediately recognize the close similarity with NAG (1.2); this would be exactly NAG if we replace $x_{k+1/2} \to x_k$ in the third update above. As we will show next, this small difference has actually profound consequences. Intuitively, by rolling this last update back one introduces a spurious friction into the method, as we will show through a symplectic perspective (Theorem 4.2 below). The method (4.3) is actually a second order accurate version of (4.1). In order to analyze the symplectic structure, one must work on the phase space (x, p). The true phase space equivalent to NAG is given by

$$x_{k+1/2} = x_k + \tfrac{h}{m} e^{-\gamma h} p_k, \quad p_{k+1} = e^{-\gamma h} p_k - h \nabla f(x_{k+1/2}), \quad x_{k+1} = x_k + \tfrac{h}{m} p_{k+1}, \tag{4.6}$$

which is completely equivalent to (1.2) under the correspondence (4.2). We thus have the following.

Theorem 4.2. *Nesterov's accelerated gradient* (1.2)*, or equivalently* (4.6)*, is an integrator of order $r = 1$ to the Hamiltonian system* (2.2)*. This method is not conformal symplectic, and rather contracts the symplectic form as*

$$\omega_{k+1} = e^{-\gamma h} \left[I - \tfrac{h^2}{m} \nabla^2 f(x_k) \right] \omega_k + O(h^3). \tag{4.7}$$

Proof. The details are presented in Appendix B, but the argument is simple. First, compare Taylor expansions of (4.6) and $(x(t+h), p(t+h))$. Second, use the variational form of (4.6), replace into $dx_{k+1} \wedge dp_{k+1}$, and then use basic properties of the wedge product (bilinearity and antisymmetry). □

Alternative form It is perhaps more common to find NAG in an alternative form:

$$x_{k+1} = y_k - \epsilon \nabla f(y_k), \qquad y_{k+1} = x_{k+1} + \mu_{k+1}(x_{k+1} - x_k), \tag{4.8}$$

where $\mu_{k+1} = k/(k+3)$. This is equivalent to (1.2) as can be seen by introducing the variable $v_k \equiv x_k - x_{k-1}$ and writing the updates in terms of x and v. When μ_k is constant, Theorem 4.2 shows that the method is not conformal symplectic. When $\mu_k = k/(k+3)$, the differential equation associated to (4.8) is equivalent to (2.1)/(2.2) with $\gamma = 3/t$. It is possible to generalize the above results for time dependent cases [18], therefore, also in this case, NAG does not preserve the symplectic structure of the system; we note that (4.7) still holds with $e^{-\gamma h} \to e^{-3\log(1+h/t_k)}$ where $t_k = hk$.

Preserving stability and continuous rates An important question is whether being symplectic is beneficial or not for optimization. Very recently, it has been shown [18] that symplectic discretizations may indeed preserve continuous-time rates of convergence when f is smooth and the system is appropriately dampened (choice of γ)—the continuous rates can be obtained via Lyapunov analysis. Thus, assuming we have a suitable conformal Hamiltonian system, conformal symplectic integrators provide a principled approach to construct optimization algorithms which are guaranteed to respect the main properties of the system such as stability of critical points and convergence rates. Furthermore, we claim that there is a delicate tradeoff where being conformal symplectic is related to an improved stability, in the sense that the method can operate with larger step sizes, while the spurious dissipation introduced by NAG (Theorem 4.2) may improve the convergence rate slightly, since it introduces more contraction, but at the cost of making the method less stable. Due to the lack of space, we defer these details to Appendix C. In Appendix B we also provide important additional insights into CM and NAG, such as their associated modified or perturbed equations—which describe these methods to a higher degree of resolution—and their *shadow Hamiltonians*.

5 Dissipative Relativistic Optimization

Let us briefly mention some simple but fundamental concepts to motivate our approach. The previous algorithms are based on (2.2) which leads to a classical Newtonian system. Here, time is just a parameter that is independent of the Euclidean space $\mathbb{R}^n$ where trajectories live. This implies that there is no restriction on the speed, $\|v\| = \|dx/dt\|$, that a particle can attain. This translates to a discrete-time algorithm, such as (4.1), where large gradients ∇f give rise to a large momenta p, implying that the updates for x can diverge. On the other hand, in special relativity, space and time form a unified geometric entity, the $(n+1)$-dimensional Minkowski spacetime with coordinates $X = (ct; x)$, where c is the speed of light. An infinitesimal distance on this manifold is given by $ds^2 = -(cdt)^2 + \|dx\|^2$. Null geodesics correspond to $ds^2 = 0$, implying $\|v\|^2 = \|dx/dt\|^2 = c^2$, i.e., no particle can travel faster than c. This imposes constraints on the geometry where trajectories take place—it is actually a hyperbolic geometry. With that being said, the idea is that by discretizing a relativistic system we can incorporate these features into an optimization algorithm, which may bring benefits such as an improved stability.

A relativistic particle subject to a potential f is described by the Hamiltonian [33]:

$$H(x,p) = c\sqrt{\|p\|^2 + m^2c^2} + f(x). \tag{5.1}$$

In the classical limit, $\|p\| \ll mc$, one obtains $H = mc^2 + \|p\|^2/(2m) + f(x) + O(1/c^2)$, recovering (2.2) up to the—notorious—constant $E_0 = mc^2$, which has no effect in deriving the equations of motion. Replacing (5.1) into (2.1) we thus obtain a *dissipative relativistic system*:

$$\dot{x} = c\,p/\sqrt{\|p\|^2 + m^2c^2}, \qquad \dot{p} = -\nabla f - \gamma p. \tag{5.2}$$

Importantly, in (5.2) the momentum is normalized by the $\sqrt{\cdot}$ factor so that $\dot{x}$ remains bounded even if p was to go unbounded. Now, replacing (5.1) into the first order accurate conformal symplectic integrator (3.2) we obtain:

$$p_{k+1} = e^{-\gamma h} p_k - h\nabla f(q_k), \qquad x_{k+1} = x_k + hcp_{k+1}/\sqrt{\|p_{k+1}\|^2 + m^2c^2}. \tag{5.3}$$

When $c \to \infty$ this recovers CM (4.1). Thus, this method is a relativistic generalization of CM. Moreover, (5.3) is a first order conformal symplectic integrator by construction (Theorems 3.3 and 3.4).

One can replace the Hamiltonian (5.1) into (3.3) to obtain a second order version of (5.3). However, motivated by the close connection between NAG and (4.3)—recall the comments following (4.5) about NAG "rolling back" the last update—let us additionally introduce a convex combination, $\alpha x_{k+1/2} + (1-\alpha)x_k$ where $0 \le \alpha \le 1$, between the initial and the midpoint of the method. In this manner, we can interpolate between a conformal symplectic regime and a spurious Hessian damping regime—recall Theorem 4.2. Therefore, we obtain the following integrator:

$$x_{k+1/2} = x_k + (hc/2)e^{-\gamma h/2}p_k \Big/ \sqrt{e^{-\gamma h}\|p_k\|^2 + m^2c^2}, \tag{5.4a}$$

$$p_{k+1/2} = e^{-\gamma h/2}p_k - h\nabla f(x_{k+1/2}), \tag{5.4b}$$

$$x_{k+1} = \alpha x_{k+1/2} + (1-\alpha)x_k + (hc/2)p_{k+1/2} \Big/ \sqrt{\|p_{k+1/2}\|^2 + m^2c^2}, \tag{5.4c}$$

$$p_{k+1} = e^{-\gamma h/2}p_{k+1/2}. \tag{5.4d}$$

We call this method *relativistic gradient descent* (RGD). Introducing

$$v_k \equiv \tfrac{h}{2m}p_k, \qquad \epsilon \equiv \tfrac{h^2}{2m}, \qquad \mu \equiv e^{-\gamma h}, \qquad \delta \equiv 4/(ch)^2, \tag{5.5}$$

the updates (5.4) assume the equivalent form stated in Algorithm 1 in the introduction.

RGD (5.4) (resp. Algorithm 1) has several interesting limits, recovering the behaviour of known algorithms as particular cases. For instance, when $c \to \infty$ (resp. $\delta \to 0$), it reduces to an interpolation between CM (4.1) (resp. (1.1)) and NAG (4.6) (resp. (1.2)). If we additionally set $\alpha = 0$ it becomes precisely NAG, whether when $\alpha = 1$ it becomes a second order version of CM—the dynamics of both CM and this second order version is pretty close, and if anything the latter is even more stable than the former (see Appendix C). When $\alpha = 1$, and arbitrary c (or δ), RGD is a conformal symplectic integrator thanks to Theorems 3.3. Recall also that Theorem 3.4 implies that RGD is a second order accurate integrator. When $\alpha = 0$, and arbitrary c (or δ), RGD is no longer conformal symplectic and introduces a Hessian driven damping in the spirit of NAG. Finally, the parameter c (or δ) controls the strength of the normalization term in the position updates of (5.4) (or Algorithm 1), which can help preventing divergences when navigating through a rough landscape with large gradients, or fast growing tails. Indeed, note that $\|x_{k+1} - \alpha x_{k+1/2} - (1-\alpha)x_k\| \le 1/\delta$ is always bounded for $\delta > 0$; this becomes unbounded when $\delta \to 0$, i.e. in the classical limit of CM and NAG.

In short, RGD is a novel algorithm with quite some flexibility and unique features, generalizing perhaps the two most important accelerated gradient-based methods in the literature—which can be recovered as limiting cases. Next, we illustrate numerically through simple yet insightful examples that RGD can be more stable and faster than CM and NAG.

6 Numerical Experiments

Let us compare RGD as given in Algorithm 1 against NAG (1.2) and CM (1.1) on some test problems. We stress that all hyperparameters of each of these methods were systematically optimized through Bayesian optimization [34] (the default implementation uses a Tree of

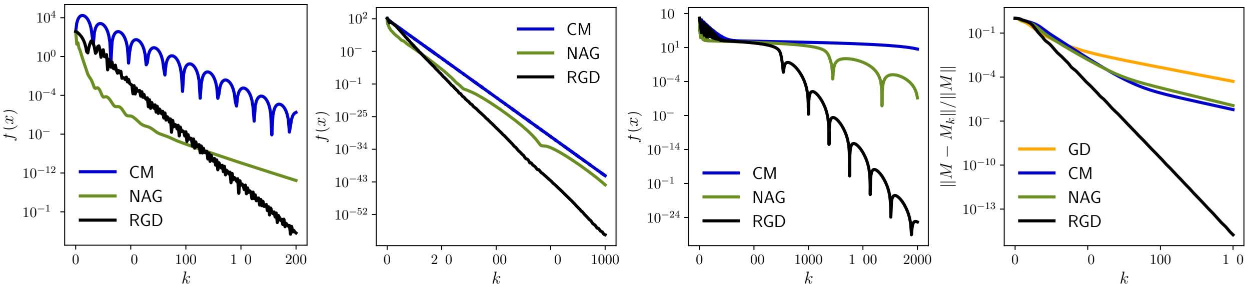

(a) Correlated quadratic (b) Random quadratic (c) Rosenbrock (d) Matrix completion

Figure 1: Convergence rate showing improved performance of RGD (Algorithm 1); see text.

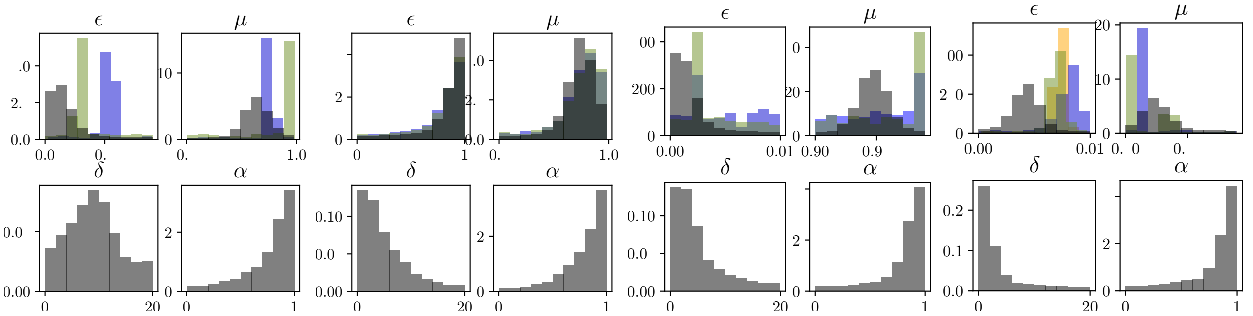

(a) Correlated quadratic (b) Random quadratic (c) Rosenbrock (d) Matrix completion

Figure 2: Histograms of hyperparameter tuning by Bayesian optimization related to Fig. 1. Tendency towards $\alpha \approx 1$ indicates benefits of being symplectic, while $\alpha \approx 0$ of being extra damped as in NAG. Tendency towards $\delta > 0$ indicates benefits of relativistic normalization. (Color line follows Fig. 1.)

Parzen estimators). This yields optimal and unbiased parameters automatically. Moreover, by checking the distribution of these hyperparameters during the tuning process we can get intuition on the sensitivity of each method. Thus, for each algorithm, we show its convergence rate in Fig. 1 when the best hyperparameters are used. In addition, in Fig. 2 we show the distribution of hyperparameters during the Bayesian optimization step—the parameters are indicated and color lines follow Fig. 1. Such values are obtained only when the respective algorithm was able to converge. We note that usually CM and NAG diverged more often than RGD which seemed more robust to parameter choice. Below we describe the optimization problems where such algorithms were tested over.

Correlated quadratic Consider $f(x) = (1/2)x^T Q x$ where $Q_{ij} = \rho^{|i-j|}$, $\rho = 0.9$, and Q has size 50×50—this function was also used in [14]. We initialize at $x_0 = (1, \ldots, 1)$ and $v_0 = 0$. The convergence results are in Fig. 1a. The distribution of parameters during tuning is in Fig. 2a, showing that $\alpha \to 1$ is preferable. This gives evidence for an advantage in being conformal symplectic in this case. Note also that $\delta > 0$, thus "relativistic effects" played an important role to improve convergence.

Random quadratic Consider $f(q) = (1/2)x^T Q x$ where Q is a 500×500 positive definite random matrix with eigenvalues uniformly distributed in $[10^{-3}, 1]$. Convergence rates are in Fig. 1b with the histograms of parameter search in Fig. 2b. Again, there is a preference in $\alpha \to 1$, evidencing benefits in being conformal symplectic. Here δ had a less important role compared to Fig. 2a.

Rosenbrock For a challenging problem in higher dimensions, consider the nonconvex Rosenbrock function $f(x) \equiv \sum_{i=1}^{n-1} \left(100(x_{i+1} - x_i^2)^2 + (1 - x_i)^2\right)$ with $n = 100$ [35, 36]; this case was already studied in detail [37]. Its landscape is quite involved, e.g. there are two minimizers: one global at $x^\star = (1, \dots, 1)^T$ with $f(x^\star) = 0$ and one local near $x \approx (-1, 1, \dots, 1)^T$ with $f \approx 3.99$. There are also—exponentially—many saddle points [37], however only two of these are actually hard to escape. These four stationary points account for 99.9% of the solutions found by Newton's method [37]. We note that both minimizers lie on a flat, deep, and narrow valley, making optimization challenging. In Fig. 1c we have the convergence of each method initialized at $x_{0,i} = \pm 2$ for i odd/even. Fig. 2c shows histograms for parameter selection. Again, we see the favorable symplectic tendency, $\alpha \to 1$, and relativistic effects, $\delta \neq 0$, played a predominant role to improve convergence.

Matrix completion Consider an $n \times n$ matrix M of rank $r \ll n$ with observed entries in the support $(i, j) \in \Omega$, where $P_\Omega(M)_{ij} = M_{ij}$ if $(i, j) \in \Omega$ and $P_\Omega(M)_{ij} = 0$ projects onto this support. The goal is to recover M from the knowledge of $P_\Omega(M)$. We assume that the rank r is known. In this case, if the number of observed entries is $O(rn)$ it is possible to recover M with high probability [38]. We do this by solving the nonconvex problem $\min_{U,V} \|P_\Omega(M - UV^T)\|_F^2$, where $U, V \in \mathbb{R}^{n \times r}$, by alternating minimization: for each iteration we apply the previous algorithms first on U with V held fixed, followed by similar updates for V with the new U fixed. This is a know technique for gradient descent (GD) which we additionally include as a baseline. We generate $M = RS^T$ where $R, S \in \mathbb{R}n \times r$ have i.i.d entries from the normal distribution $\mathcal{N}(1, 2)$. We initialize U and V sampled from the standard normal $\mathcal{N}(0, 1)$. The support is chosen uniformly at random with sampling ratio $s = 0.3$, yielding $p = sn^2$ observed entries. We set $n = 100$ and $r = 5$. This gives a number of effective degrees of freedom $d = r(2n - r)$ and the "hardness" of the problem can be quantified via $d/p \approx 0.325$. Fig. 1d shows the convergence rate, and Fig. 2d the parameter search.

7 Discussion and Outlook

This paper builds on a recent line of research connecting accelerated optimization algorithms to continuous dynamical systems. We brought *conformal symplectic* techniques for dissipative systems into this context, besides proposing a new method called *relativistic gradient descent* (RGD) based on a dissipative relativistic system; see Algorithm 1. This method generalizes both the well-know classical momentum (CM) given by (1.1), also known as heavy ball, as well as Nesterov's accelerated gradient (NAG) given by (1.2); each of these methods are recovered as particular cases from RGD, which has no additional computational cost compared to CM and NAG. Moreover, RGD has more flexibility, can interpolate between a conformal symplectic behaviour or introduce some Hessian dependent damping in the spirit of NAG, and has potential to control instabilities due to large gradients by normalizing the momentum. In our experiments, RGD significantly outperfomed CM and NAG.

We also elucidated the symplectic structure behind CM and NAG. We found that the former turns out to be a conformal symplectic integrator (Corollary 4.1), thus being "dissipative-preserving," while the latter introduces a spurious contraction of the symplectic form by a Hessian driven damping (Theorem 4.2). This is an effect of second order in the step size but may affect convergence and stability. We pointed out that there is a tradeoff between this extra contraction and the stability of a conformal symplectic method. These ideas are explored in more detail in the Appendix C. We also derive modified or perturbed equations for CM and NAG, describing these methods to a higher degree of resolution; this analysis provides several new insights into these methods that were not previously considered.

A more refined analysis of RGD is certainly an interesting future problem, although considerably challenging due to the nonlinearity introduced by the $\sqrt{1+\delta\|v\|^2}$ term in the updates of Algorithm 1. To give an example, even if one assumes a simple quadratic function $f(x) = (\lambda/2)x^2$, the differential equations (5.2) are highly nonlinear and do not admit a closed form solution, contrary to the associated differential equation associated to CM and NAG which are linear and can be readily integrated. Thus, even in continuous-time, the analysis for RGD is likely to be involved. Finally, it would be interesting to consider RGD in a stochastic setting, namely investigate its diffusive properties in a random media which may bring benefits to nonconvex optimization and sampling.

Acknowledgments

This work was supported by grants ARO MURI W911NF-17-1-0304 and NSF 1447822.

A Order of Accuracy of the General Integrators

It is known that a composition of the type $\Psi_h^A \circ \Psi_h^B$, where A and B represents the components of distinct vector fields, leads to an integrator of order $r = 1$, whereas a composition in the form $\Psi_{h/2}^A \circ \Psi_h^B \circ \Psi_{h/2}^A$ leads to an integrator of order $r = 2$ [30]—this is known as Strang splitting. However, here we provide an explicit and direct proof of these facts for the generic integrators (3.2) and (3.3), respectively.

Proof of Theorem 3.4. From the equations of motion (2.1) and Taylor expansions we have:

$$\begin{aligned} x(t_k+h) &= x + h\dot{x} + \tfrac{h^2}{2}\ddot{x} + O(h^3) \\ &= x + h\nabla_p H + \tfrac{h^2}{2}\left(\nabla^2_{xp}H\dot{x} + \nabla^2_{pp}H\dot{p}\right) + O(h^3) \\ &= x + h\nabla_p H + \tfrac{h^2}{2}\nabla^2_{xp}H\nabla_p H - \tfrac{h^2}{2}\nabla^2_{xp}\nabla_x H - \tfrac{h^2}{2}\gamma\nabla^2_{pp}Hp + O(h^3), \end{aligned} \tag{A.1}$$

and

$$\begin{aligned} p(t_k+h) &= p + h\dot{p} + \tfrac{h^2}{2}\ddot{p} + O(h^3) \\ &= p - h\nabla_x H - h\gamma p + \tfrac{h^2}{2}\left(-\nabla^2_{xx}H\dot{x} - \nabla^2_{xp}H\dot{p} - \gamma\dot{p}\right) + O(h^3) \\ &= p - h\nabla_x H - h\gamma p - \tfrac{h^2}{2}\nabla^2_{xx}H\nabla_p H + \tfrac{h^2}{2}\nabla^2_{xp}H\nabla_x H + \tfrac{h^2}{2}\gamma\nabla^2_{xx}Hp \\ &\quad + \tfrac{h^2}{2}\gamma\nabla_x H + \tfrac{h^2}{2}\gamma^2 p + O(h^3), \end{aligned} \tag{A.2}$$

where we denote $x \equiv x(t_k)$ and $p \equiv p(t_k)$ for $t_k = kh$ $(k = 0, 1, \dots)$, and it is implicit that all gradients and Hessians of H are being computed at (x, p).

Consider (3.2). Under one step of this map, starting from the point (x, p), upon using Taylor expansions we have:

$$x_{k+1} = x + h\nabla_p H + O(h^2), \tag{A.3a}$$

$$p_{k+1} = e^{-\gamma h}p - h\nabla_x H + O(h^2) = p - \gamma h p - h\nabla_x H(x, p) + O(h^2). \tag{A.3b}$$

Comparing these two equations with (A.1) and (A.2) we conclude that

$$x_{k+1} = x(t_k + h) + O(h^2), \qquad p_{k+1} = p(t_k + h) + O(h^2). \tag{A.4}$$

Therefore, the discrete state approximates the continuous-time state up to an error of $O(h^2)$, obeying Definition 3.1 with $r = 1$.

The same approach is applicable to the numerical map (3.3). Expanding the first update:

$$\begin{aligned} \tilde{X} &= x + \tfrac{h}{2}\nabla_p H\big(x + \tfrac{h}{2}\nabla_p H, p - \tfrac{h}{2}\gamma p\big) + O(h^3), \\ &= x + \tfrac{h}{2}\nabla_p H + \tfrac{h^2}{4}\nabla^2_{xp}H\nabla_p H - \tfrac{h^2}{4}\gamma\nabla^2_{pp}Hp + O(h^3). \end{aligned} \tag{A.5}$$

Expanding the second update:

$$\begin{aligned} \tilde{P} &= e^{-\gamma h/2}p - \tfrac{h}{2}\nabla_x H\big(x + \tfrac{h}{2}\nabla_p H, p - \tfrac{h}{2}\gamma p\big) \\ &\qquad - \tfrac{h}{2}\nabla_x H\big(x + \tfrac{h}{2}\nabla_p H, p - \tfrac{h}{2}\gamma p - h\nabla_x H\big) + O(h^3), \\ &= e^{-\gamma h/2}p - h\nabla_x H - \tfrac{h^2}{2}\nabla^2_{xx}H\nabla_p H + \tfrac{h^2}{2}\gamma\nabla^2_{xp}Hp + \tfrac{h^2}{2}\nabla^2_{xp}H\nabla_x H + O(h^3). \end{aligned} \tag{A.6}$$

Making use of (A.5) and (A.6) we thus find:

$$\begin{aligned} X &= \tilde{X} + \tfrac{h}{2}\nabla_p H(\tilde{X}, \tilde{P}) \\ &= x + \tfrac{h}{2}\nabla_p H + \tfrac{h^2}{4}\nabla^2_{xp}H\nabla_p H - \tfrac{h^2}{4}\gamma\nabla^2_{pp}Hp \\ &\qquad + \tfrac{h}{2}\nabla H\big(x + \tfrac{h}{2}\nabla_p H, p - \tfrac{h}{2}\gamma p - h\nabla_x H\big) + O(h^3) \\ &= x + h\nabla_p H + \tfrac{h^2}{2}\nabla^2_{xp}H\nabla_p H - \tfrac{h^2}{2}\gamma\nabla^2_{pp}Hp - \tfrac{h^2}{2}\nabla^2_{pp}H\nabla_x H + O(h^3). \end{aligned} \tag{A.7}$$

Thus, comparing with (A.1) we conclude that $x_{k+1} = x(t_k + h) + O(h^3)$. Finally, from (A.6) we have

$$
\begin{aligned}
P &= e^{-\gamma h/2}\tilde{P} \\
&= e^{\gamma h} p - e^{-\gamma h/2}\Big\{ h\nabla_x H + \tfrac{h^2}{2}\nabla^2_{xx}H\nabla_p H + \tfrac{h^2}{2}\gamma\nabla^2_{xp}Hp - \tfrac{h^2}{2}\nabla^2_{xp}H\nabla_x H\Big\} + O(h^3) \\
&= p - \gamma h p + \tfrac{h^2}{2}\gamma^2 p - h\nabla_x H - \tfrac{h^2}{2}\nabla^2_{xx}H\nabla_p H + \tfrac{h^2}{2}\gamma\nabla^2_{xp}Hp \\
&\qquad + \tfrac{h^2}{2}\nabla^2_{xp}H\nabla_x H + \tfrac{h^2}{2}\gamma\nabla_x H + O(h^3).
\end{aligned} \tag{A.8}
$$

Comparing this with (A.2) implies $p_{k+1} = p(t_k + h) + O(h^3)$. Therefore, in this case we satisfy Definition 3.1 with $r = 2$. □

From the above general results it is immediate that:

- CM given by (1.1)—or equivalently written in the form (4.1) which is more appropriate to make connections with the associated continuous system—is a first order integrator to the conformal Hamiltonian system (2.1) with the classical Hamiltonian (2.2) (the equations of motion are (B.2) below).
- The relativistic extension of CM given by (5.3) is a first order integrator to the conformal relativistic Hamiltonian system (5.2).
- RGD given by (5.4) with $\alpha = 1$—also equivalently written in the form of Algo. 1—is a second order integrator to (5.2).

B Insights into Nesterov and Heavy Ball Methods

Here we prove Theorem 4.2 but additionally provide several other details which give insights into Nesterov's method (NAG) and heavy ball or classical momentum (CM), such as their underlying "modified equations" and "shadow Hamiltonians."

B.1 Order of Accuracy

We work on phase space variables (x, p), thus NAG should be considered in the form (4.6), which we repeat below for convenience:

$$x_{k+1/2} = x_k + \tfrac{h}{m}e^{-\gamma h}p_k, \tag{B.1a}$$

$$p_{k+1} = e^{-\gamma h}p_k - h\nabla f(x_{k+1/2}), \tag{B.1b}$$

$$x_{k+1} = x_k + \tfrac{h}{m}p_{k+1}. \tag{B.1c}$$

Recall that this is precisely (1.2) under the change of variables (4.2). Let us now derive the order of accuracy of this method with respect to its underlying continuous Hamiltonian system (2.1) with Hamiltonian (2.2):

$$\dot{x} = p/m, \qquad \dot{p} = -\nabla f(x) - \gamma p. \tag{B.2}$$

Proof of Theorem 4.2, part (i). Denoting $x = x(t_k)$ and $p = p(t_k)$, we expand the exponential in (B.1a) to obtain

$$x_{k+1/2} = x + \tfrac{h}{m} p - \tfrac{h^2}{m} \gamma p + O(h^3). \tag{B.3}$$

Using this and Taylor expansions in the last two updates (B.1b) and (B.1c):

$$\begin{aligned} p_{k+1} &= p - h\gamma p - h\nabla f(x) + \tfrac{h^2}{2}\gamma^2 p - \tfrac{h^2}{m}\nabla^2 f(x) p_k + O(h^3), && \text{(B.4a)} \\ x_{k+1} &= x + \tfrac{h}{m} p - \tfrac{h^2}{m}\gamma p - \tfrac{h^2}{m}\nabla f(x) + O(h^3). && \text{(B.4b)} \end{aligned}$$

It is implicit that ∇f and $\nabla^2 f$ are computed at (x, p). From the equations of motion (B.2), i.e. replacing the Hamiltonian (2.2) into the general approximations (A.1) and (A.2), we obtain:

$$\begin{aligned} p(t_k + h) &= p - h\nabla f - h\gamma p - \tfrac{h^2}{2m}\nabla^2 f p + \tfrac{h^2}{2}\gamma \nabla^2 f p + \tfrac{h^2}{2}\gamma\nabla f + \tfrac{h^2}{2}\gamma^2 p + O(h^3), && \text{(B.5a)} \\ x(t_k + h) &= x + \tfrac{h}{m} p - \tfrac{h^2}{2m}\gamma p + O(h^3). && \text{(B.5b)} \end{aligned}$$

Hence, by comparison with (B.4) we have $x_{k+1} = x(t_k + h) + O(h^2)$ and $p_{k+1} = p(t_k + h) + O(h^2)$, which according to Definition 3.1 means that NAG is an integrator of order $r = 1$, as claimed. □

Thus both NAG and CM are first order integrators to (B.2). We already know that CM is conformal symplectic.

B.2 Spurious Contraction of the Symplectic Form

Next, we consider how NAG changes the symplectic structure of the underlying conformal Hamiltonian system.

Proof of Theorem 4.2, part (ii). Consider the variational form of (B.1) (the notation is standard in numerical analysis [30]):

$$\begin{aligned} dx_{k+1/2} &= dx_k + \tfrac{h}{m} e^{-\gamma h} dp_k, && \text{(B.6a)} \\ dp_{k+1} &= e^{-\gamma h} dp_k - h\nabla^2 f(x_{k+1/2}) dx_{k+1/2}, && \text{(B.6b)} \\ dx_{k+1} &= dx_k + \tfrac{h}{m} dp_{k+1}. && \text{(B.6c)} \end{aligned}$$

Using these, bilinearity and the antisymmety of the wedge product, together the fact that $\nabla^2 f$ is symmetric, we obtain:

$$\begin{aligned} dx_{k+1} \wedge dp_{k+1} &= dx_k \wedge dp_{k+1} \\ &= e^{-\gamma h} dx_k \wedge dp_k - h dx_k \wedge \nabla^2 f\big(x_{k+1/2}\big) dx_{k+1/2} \\ &= e^{-\gamma h} dx_k \wedge dp_k - \tfrac{h^2}{m} e^{-\gamma h} dx_k \wedge \nabla^2 f(x_{k+1/2}) dp_k \\ &= e^{-\gamma h} dx_k \wedge dp_k - \tfrac{h^2}{m} e^{-\gamma h} dx_k \wedge \nabla^2 f(x_k) dp_k + O(h^3), \end{aligned} \tag{B.7}$$

where in the last passage we used a Taylor approximation for $x_{k+1/2}$. Thus, $dx_{k+1} \wedge dp_{k+1} \neq e^{-\gamma h} dx_k \wedge dp_k$, showing that the method is not conformal symplectic (see Definition 3.2). Moreover, using the symmetry of $\nabla^2 f$ we can write (B.7) as

$$\omega_{k+1} = e^{-\gamma h} \left[I - \tfrac{h^2}{m} \nabla^2 f(x_k) \right] \omega_k + O(h^3), \tag{B.8}$$

which is exactly (4.7). □

Thus, while CM exactly preserve the same dissipation found in the continuous-time system, NAG introduces some extra contraction or expansion of the symplectic form, depending whether $\nabla^2 f$ is positive definite or not. From (B.8), in k iterations of NAG, and neglecting the $O(h^3)$ error term, we have:

$$\begin{aligned} \omega_k &\approx e^{-\gamma t_k} \prod_{i=1}^{k} \left[I - \tfrac{h^2}{m} \nabla^2 f(x_{k-i}) \right] \omega_0 \\ &\approx e^{-\gamma t_k} \left[I - \tfrac{h^2}{m} \big(\nabla^2 f(x_{k-1}) - \nabla^2 f(x_{k-2}) - \cdots - \nabla^2 f(x_0) \big) \right] \omega_0. \end{aligned} \tag{B.9}$$

This depends on the entire history of the Hessians from the initial point. Therefore, NAG contracts the symplectic form slightly more than the underlying conformal Hamiltonian system—assuming $\nabla^2 f$ is positive definite—and it does so in a way that depends on the Hessian of the objective function. Note that this is a small effect of $O(h^2)$. Moreover, if $\nabla^2 f$ has negative eigenvalues, e.g. f is nonconvex and has saddle points, then NAG actually introduces some spurious excitation in that direction. To gain some intuition, let us consider the simple case of a quadratic function:[4]

$$f(x) = (\lambda/2) x^2 \tag{B.10}$$

for some constant λ. Thus (B.8) becomes

$$\omega_{k+1} \approx e^{-\gamma h + \log(1 - h^2 \lambda/m)} \omega_k \approx e^{-(\gamma + h\lambda/m) h} \omega_k \qquad \Longrightarrow \qquad \omega_k \approx e^{-(\gamma + h\lambda/m) t_k} \omega_0. \tag{B.11}$$

This suggests that effectively the original damping of the system is being replaced by $\gamma \to \gamma + h\lambda/m$. Thus if $\lambda > 0$ there is some spurious damping, whereas if $\lambda < 0$ there is some spurious excitation.

[4] This quadratic function is actually enough to capture the behaviour when close to a critical point $x^\star$ since $f(x) \approx f(x^\star) + \frac{1}{2} \nabla^2 f(x^\star) x$ and one can work on rotated coordinates where $\nabla^2 f(x^\star) = \operatorname{diag}(\lambda_1, \ldots, \lambda_n)$.

B.3 Modified Equations and Shadow Hamiltonian

We have seen above that NAG is a first order integrator to the conformal Hamiltonian system (B.2), however it changes slightly the behaviour of the original system since it introduces spurious damping/excitation. To understand its behaviour more closely, one can ask the following question: *for which continuous dynamical system NAG turns out to be a second order integrator?* In other words, we can look for a modified system that captures the behaviour of NAG more closely, up to $O(h^3)$. Every numerical method is known to have a modified or perturbed differential equation [30] (the brief discussion in [18] may also be useful). With respect to this question, we thus find the following.

Theorem B.1 (Shadow dynamical system for Nesterov's method)**.** *NAG* (1.2)*, or its equivalent phase space representation* (B.1)*, is a second order integrator to the following modified or perturbed equations:*

$$\dot{x} = \frac{p}{m} - \frac{\gamma h}{2m} p - \frac{h}{2m}\nabla f(x), \qquad \dot{p} = -\nabla f(x) - \gamma p - \frac{h\gamma}{2}\nabla f - \frac{h}{2m}\nabla^2 f(x) p. \tag{B.12}$$

Proof. We look for vector fields $F(q,p;h)$ and $G(q,p;h)$ for the modified system

$$\dot{x} = p/m + hF, \qquad \dot{p} = -\nabla f(x) - \gamma p - hG, \tag{B.13}$$

such that (B.1) is an integrator of order $r=2$. This can be done by computing [30]:

$$F = \lim_{h\to 0} \frac{x_{k+1} - x(t_k+h)}{h^2}, \qquad G = \lim_{h\to 0} \frac{p_{k+1} - p(t_k+h)}{h^2}. \tag{B.14}$$

From (B.4) and (B.5) we obtain precisely (B.12). By the previously discussed approach through Taylor expansions one can also readily check that NAG is indeed an integrator of order $r=2$ to this perturbed system. □

We can also combine (B.12) into a second order differential equation:

$$m\ddot{x} + m\left(\gamma I + \frac{h}{m}\nabla^2 f(x)\right)\dot{x} = -\left(I + \frac{h\gamma}{2}I - \frac{h^2\gamma^2}{4}I + \frac{h^2}{4m}\nabla^2 f(x)\right)\nabla f(x), \tag{B.15}$$

where I is the $n\times n$ identity matrix. We see that this equation has several new ingredients compared to $\ddot{x} + \gamma\dot{x} = -(1/m)\nabla f(x)$ which is obtained from (B.2). First, when $h\to 0$ the system (B.15) tends to the latter, as it should since both must agree to leading order. Second, the spurious change in the damping coefficient reflects the behaviour of the symplectic form (B.8) (see also (B.11)). Third, we see that the gradient ∇f is rescaled by the contribution of several terms, including the Hessian, making explicit a curvature dependent behaviour, which also appears in the damping coefficient. Note that the modified equation (B.15), or equivalently (B.12), depends on the step size h. It therefore captures an intrinsic behaviour of the discrete-time algorithm which is not captured by (B.2).

Since CM is also a 1st order integrator to (B.2), which is actually conformal symplectic, it is natural to consider its modified equation and compare with the one for NAG (B.12).

Theorem B.2 (Shadow Hamiltonian for Heavy Ball)**.** *Heavy ball or CM method* (1.1)*, equivalently written in phase space as* (4.1)*, is a second order integrator to the following modified conformal Hamiltonian system:*

$$\dot{x} = \frac{p}{m} - \frac{h\gamma}{2m}p - \frac{h}{2m}\nabla f(x), \qquad \dot{p} = -\nabla f(x) - \gamma p - \frac{h\gamma}{2}\nabla f(x) + \frac{h}{2m}\nabla^2 f(x) p. \tag{B.16}$$

Such a system admits the shadow or perturbed Hamiltonian

$$\tilde{H} = \frac{\|p\|^2}{2m} + f(x) - \frac{h\gamma}{4m}\|p\|^2 - \frac{h}{2m}\langle \nabla f(x), p\rangle + \frac{h\gamma}{2}f. \tag{B.17}$$

Proof. Exactly as in Theorem B.1. One can readily verify that replacing (B.17) into (2.1) gives (B.17). □

We note the striking similarity between (B.16) and (B.12); the only difference is the sign of the last term in the momentum equation. Up to this level of resolution, the difference is that NAG introduces a spurious damping compared to CM, in agreement with the derivation of the symplectic form (B.8). On the other hand, notice that the perturbed system (B.16) for CM is conformal Hamiltonian, contrary to (B.12) that cannot be written in Hamiltonian form; this is the reason why structure-preserving discretizations tend to be more stable since the perturbed trajectories are always close—i.e., within a bounded error—from the original Hamiltonian dynamics. We can also combine (B.16):

$$m\ddot{x} + m\gamma\dot{x} = -\left(I + \frac{h\gamma}{2}I - \frac{h^2\gamma^2}{4}I - \frac{h^2}{4m}\nabla^2 f(x)\right)\nabla f(x). \tag{B.18}$$

Again, this is strikingly similar to (B.15). Note that this equation does not have the spurious damping term $(h/m)\nabla^2 f(x)$ as in (B.15), i.e., it preserves exactly the dissipation in the original continuous system. As we will show below, there is a balance between preserving the dissipation of the original system and stability. While NAG introduces an extra damping, and may slightly help in an improved convergence since it dissipates more energy, this comes at a cost of a lack in stability.

C Tradeoff Between Stability and Convergence Rate

Here we illustrate an interesting phenomenon: there is a tradeoff between stability versus convergence rate. Intuitively, an improved rate is associated to a higher "contraction," i.e. the introduction of spurious dissipation in the numerical method. However, this makes the method less stable, and ultimately very sensitive to parameter tuning. On the other hand, a geometric or structure-preserving integrator may have slightly less contraction, since it preserves the original dissipation of the continuous system exactly, but it is more stable and able to operate with larger step sizes. Furthermore, a structure-preserving method is guaranteed to reproduce very closely, perhaps even up to a negligible error, the continuous-time rates of convergence [18]. This indicates that there may have benefits in considering this class of methods for optimization, such as conformal symplectic integrators that are being advocated in this paper.

Stability of a numerical integrator means the region of hyperparameters, e.g., values of the step size, such that the method is able to converge. The larger this region, more stable is the method. The convergence rate is a measure of how fast the method tends to the minimum, and this is related to the amount of contraction between subsequent states or subsequent values of the objective function. For instance, since NAG introduces some spurious dissipation—recall (B.8)—we expect that it may have a slightly higher contraction compared to CM, which exactly preserves the dissipation of the continuous system. Thus, such a spurious dissipation can induce a slightly improved convergence rate, but as we will show below at the cost of making the method more unstable and thus requiring smaller step sizes.

Let us consider a standard linear stability analysis, which involves a quadratic function (B.10) such that the previous methods can be treated analytically. Thus, replacing (B.10) into CM in the form (4.1) it is possible to write the algorithm as a linear system:

$$z_{k+1} = T_{\text{CM}} z_k, \qquad T_{\text{CM}} = \begin{bmatrix} 1 - h^2\lambda/m & (h/m)e^{-\gamma h} \\ -h\lambda & e^{-\gamma h} \end{bmatrix}, \tag{C.1}$$

where we denote $z = \left[\begin{smallmatrix} x \\ p \end{smallmatrix}\right]$. Similarly, NAG in the form (4.6) yields

$$z_{k+1} = T_{\text{NAG}} z_k, \qquad T_{\text{NAG}} = \begin{bmatrix} 1 - h^2\lambda/m & (h/m)e^{-\gamma h}(1 - h^2\lambda/m) \\ -h\lambda & e^{-\gamma h}(1 - h^2\lambda/m) \end{bmatrix}, \tag{C.2}$$

while RGD (5.4), with $c \to \infty$ and $\alpha = 1$, yields[5]

$$z_{k+1} = T_{\text{RGD}} z_k, \qquad T_{\text{RGD}} = \begin{bmatrix} 1 - h^2\lambda/(2m) & h/(2m)e^{-\gamma h/2}(2 - h^2\lambda/(2m)) \\ -h\lambda e^{-\gamma h/2} & e^{-\gamma h}(1 - h^2\lambda/(2m)) \end{bmatrix}. \tag{C.3}$$

A linear system is stable if the spectral radius of its transition matrix is $\rho(T) \le 1$. We can compute the eigenvalues of the above matrices and check for which range of parameters they remain inside the unit circle; e.g., for given γ, m, and λ we can find the allowed range of the step size h for which the maximum eigenvalue in absolute value is $|\lambda_{\max}| \le 1$. Instead of showing the explicit formulas for these eigenvalues, which can be obtained quite simply but are cumbersome, let us illustrate what happens graphically.

In Fig. 3, the shaded gray area represents the unit circle. Any eigenvalue that leaves this area makes the associated algorithm unstable. Here we fix $m = \lambda = \gamma = 1$ (other choices are equivalent) and we vary the step size $h > 0$. These eigenvalues are in general complex and

[5] The case of finite c is nonlinear and not amenable to such an analysis. However, this $c \to \infty$ already provide useful insights.

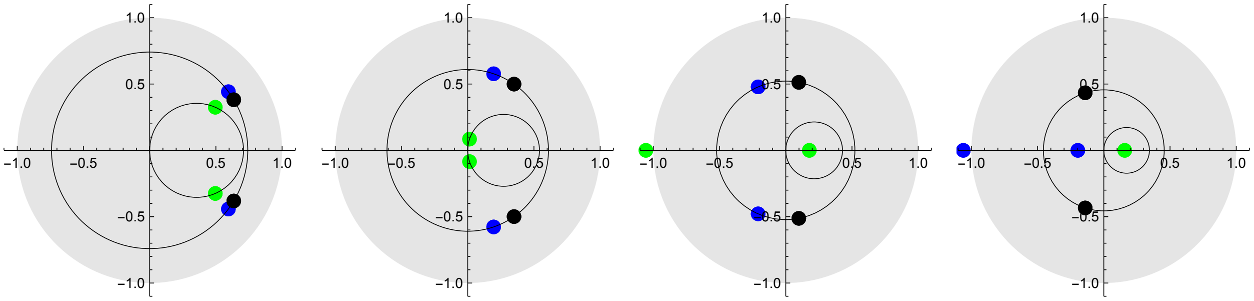

Figure 3: Stability of CM (4.1) (*blue*), NAG (4.6) (*green*), and RGD (5.4) with $c \to \infty$ and $\alpha = 1$ (*black*)—in this case it becomes a dissipative version of the Leapfrog to system (B.2). We plot the eigenvalues in the complex plane; x-axis is the real part, y-axis is the imaginary part. The unit circle represent the stability region, i.e. once an eigenvalue leaves the gray area the corresponding method becomes unstable. Both CM and RGD are symplectic thus their eigenvalues always move on a circle of radius $e^{-\gamma h/2}$ centered at the origin. NAG has eigenvalues in the smaller circle with radius $1/(e^{\gamma h}+1)$ and centered at $1/(e^{\gamma h}+1)$ on the x-axis; the circle is dislocated from the origin precisely due to spurious dissipation. From left to right we increase the step size h while keeping γ, m, and λ fixed. As h increases the eigenvalues move on the circles in the counterclockwise direction until they fall on the real line. Eventually they leave the unit circle and the associated method becomes unstable. Note how CM has higher stability than NAG, and RGD has even higher stability than CM.

they lie on a circle which is determined by the amount of friction in the system. Note how for CM and RGD this circle is centered at the origin, with radius $\sqrt{\mu} \equiv e^{-\gamma h/2}$, since these methods are conformal symplectic and exactly preserve the dissipation of the underlying continuous system. However, NAG introduces a spurious damping which is reflected as the circle being translated from the center, at a distance $1/(e^{\gamma h}+1)$, and moreover this circle has a smaller radius of $1/(e^{\gamma h}+1)$ compared to CM and RGD; since this radius is smaller in the case of RGD, it may have a faster convergence rate compared to CM and NAG when these eigenvalues are complex. As we increase h (left to right in Fig. 3), the eigenvalues move counterclockwise on the circles until falling on the real line, where one of them goes to the left while the other goes to the right. Eventually, the leftmost eigenvalue leaves the unit circle for a large enough h (third panel in Fig. 3). Note that NAG becomes unstable first, followed by CM, and only then by RGD. The main point is that CM and RGD can still be stable for much larger step sizes compared to NAG, and RGD is even more stable than CM as seen in the rightmost plot in Fig. 3; this is a consequence of RGD being an integrator of order $r = 2$ whereas CM is of order $r = 1$—besides being structure-preserving. Hence, even though NAG may have a slightly faster convergence (due to a stronger contraction), it requires a smaller step sizes and its stability is more sensitive compared to a conformal symplectic method. On the other hand, both CM and RGD can operate with larger step sizes, which in practice may even result in a faster solver compared to NAG.

To provide a more quantitative statement, after computing the eigenvalues of the above transition matrices for given $\mu \equiv e^{-\gamma h}$, m, and λ, we find the following threshold for stability:

$$h_{\mathrm{CM}} \leq \sqrt{m(1+\mu+\mu^2+\mu^3)}/(\mu\sqrt{\lambda}), \tag{C.4}$$

$$h_{\mathrm{NAG}} \leq \sqrt{m(1+\mu+\mu^2+\mu^3)}/\sqrt{\mu\lambda(1+\mu+\mu^2)}, \tag{C.5}$$

$$h_{\mathrm{RGD}} \leq \sqrt{2m(1+\mu+\mu^2+\mu^3)}/\sqrt{\mu\lambda(1+\mu)}. \tag{C.6}$$

We can clearly see that RGD has the largest region for h, followed by CM, then by NAG.

References

[1] B. T. Polyak, "Some methods of speeding up the convergence of iteration methods," *USSR Comp. Math. and Math. Physics* **4** no. 5, (1964) 1–17.

[2] Y. Nesterov, "A method of solving a convex programming problem with convergence rate $O(1/k^2)$," *Dokl. Akad. Nauk SSSR* **269** (1983) 543–547.

[3] I. Sutskever, J. Martens, G. Dahl, and G. Hinton, "On the importance of initialization and momentum in deep learning," in *Int. Conf. Machine Learning*. 2013.

[4] T. Tieleman and G. Hinton, "Lecture 6.5-RMSprop: Divide the gradient by a running average of its recent magnitude." Coursera: Neural Networks for Machine Learning, 2012.

[5] D. P. Kingma and J. L. Ba, "Adam: A method for stochastic optimization," in *Int. Conf. Learning Representations*. 2015.

[6] J. Duchi, E. Hazan, and Y. Singer, "Adaptive subgradient methods of online learning and stochastic optimization," *J. Machine Learning Research* **12** (2017) 2121–2159.

[7] T. Dozat, "Incorporating nesterov momentum into adam," in *Int. Conf. Learning Representations, Workshop*. 2016.

[8] W. Su, S. Boyd, and E. J. Candès, "A differential equation for modeling Nesterov's accelerated gradient method: Theory and insights," *J. Machine Learning Research* **17** no. 153, (2016) 1–43.

[9] A. Wibisono, A. C. Wilson, and M. I. Jordan, "A variational perspective on accelerated methods in optimization," *Proc. Nat. Acad. Sci.* **113** no. 47, (2016) E7351–E7358.

[10] W. Krichene, A. Bayen, and P. L. Bartlett, "Accelerated mirror descent in continuous and discrete time," in *Advances in Neural Information Processing Systems*, vol. 28. 2015.

[11] J. Zhang, A. Mokhtari, S. Sra, and A. Jadbabaie, "Direct Runge-Kutta discretization achieves acceleration," in *Advances in Neural Information Processing Systems*, vol. 31. 2018.

[12] B. Shi, S. S. Du, M. I. Jordan, and W. J. Su, "Understanding the acceleration phenomenon via high-resolution differential equations." arXiv:1810.08907 [math.OC], 2018.

[13] L. F. Yang, R. Arora, V. Braverman, and T. Zhao, "The physical systems behind optimization algorithms," in *Advances on Neural Information Processing Systems*. 2018.

[14] M. Betancourt, M. I. Jordan, and A. C. Wilson, "On symplectic optimization," `arXiv:1802.03653 [stat.CO]`.

[15] G. França, D. P. Robinson, and R. Vidal, "ADMM and accelerated ADMM as continuous dynamical systems," *Int. Conf. Machine Learning* (2018) .

[16] G. França, D. P. Robinson, and R. Vidal, "A nonsmooth dynamical systems perspective on accelerated extensions of ADMM," `arXiv:1808.04048 [math.OC]`.

[17] G. França, M. I. Jordan, and R. Vidal, "Gradient flows and accelerated proximal splitting methods," `arXiv:1908.00865 [math.OC]`.

[18] G. França, M. I. Jordan, and R. Vidal, "On dissipative symplectic integration with applications to gradient-based optimization," `arXiv:2004.06840 [math.OC]`.

[19] R. I. McLachlan and G. R. W. Quispel, "Geometric integrators for ODEs," *J. Phys. A: Math. Gen.* **39** (2006) 5251–5285.

[20] E. Forest, "Geometric integration for particle accelerators," *J. Phys. A: Math. Gen.* **39** (2006) 5321–5377.

[21] P. J. Channell and C. Scovel, "Symplectic integration of Hamiltonian systems," *Nonlinearity* **3** (1990) 231–259.

[22] R. Quispel and R. McLachlan, "Geometric numerical integration of differential equations," *J. Phys. A: Math. Gen.* **39** (2006) .

[23] R. McLachlan and M. Perlmutter, "Conformal Hamiltonian systems," *Journal of Geometry and Physics* **39** (2001) 276–300.

[24] A. Bhatt, D. Floyd, and B. E. Moore, "Second order conformal symplectic schemes for damped hamiltonian systems," *Journal of Scientific Computing* **66** (2016) 1234–1259.

[25] M. Muehlebach and M. I. Jordan, "Optimization with momentum: Dynamical, control-theoretic, and symplectic perspectives," `arXiv:2002.12493 [math.OC]`.

[26] X. Lu, V. Perrone, L. Hasenclever, Y. W. Teh, and S. J. Vollmer, "Relativistic monte carlo," *20th Int. Conf. Articial Intelligence and Statistics* (2017) .

[27] S. Livingstone, M. F. Faulkner, and G. O. Roberts, "Kinetic energy choice in Hamiltonian/hybrid Monte Carlo," arXiv:1706.02649 [stat.CO].

[28] C. J. Maddison, D. Paulin, Y. W. Teh, B. O'Donoghue, and A. Doucet, "Hamiltonian descent methods," arXiv:1809.05042 [math.OC].

[29] H. Flanders, *Differential Forms with Applications to the Physical Sciences.* Dover, 1989.

[30] E. Hairer, C. Lubich, and G. Wanner, *Geometric Numerical Integration.* Springer, 2006.

[31] U. Dessler, "Symmetry property of the Lyapunov spectra of a class of dissipative dynamical systems with viscous damping," *Phys. Rev. A* **38** (1988) 2103.

[32] S. Marò and A. Sorrentino, "Aubry-Mather theory for conformally symplectic systems," *Commun. Math. Phys.* **354** (2017) 775–808.

[33] L. D. Landau and E. M. Lifshitz, *The Classical Theory of Fields.* Butterworth-Heinemann, 1976.

[34] J. Bergstra, D. Yamins, and D. D. Cox, "Making a science of model search: Hyperparameter optimization in hundreds of dimensions for vision architectures," *Int. Conf. Machine Learning* (2013) .

[35] H. H. Rosenbrock, "An automatic method for finding the greatest or least value of a function," *The Computer Journal* **3** no. 3, (1960) 175–184.

[36] D. E. Goldberg, *Genetic Algorithms in Search, Optimization and Machine Learning.* Addison-Wesley, 1989.

[37] S. Kok and C. Sandrock, "Locating and characterizing the stationary points of the extended Rosenbrock function," *Evolutionary Computation* **17** no. 3, (2009) 437–453.

[38] R. H. Keshavan, A. Montanari, and S. Oh, "Matrix completion from a few entries," *IEEE Trans. Information Theory* **56** (2009) .